IET Microwaves, Antennas & Propagation

Research Article

IET Journals
The Institution of Engineering and Technology

High-isolation microstrip patch array antenna for single channel full duplex communications

ISSN 1751-8725
Received on 15th September 2014
Revised on 4th February 2015
Accepted on 4th February 2015
doi: 10.1049/iet-map.2014.0624
www.ietdl.org

Ariunzaya Batgerel[1], *Soon Young Eom*[2] ✉

[1]*Department of Mobile Communication and Digital Broadcasting Technology, University of Science and Technology, 217 Gajeongno, Yuseong-gu, Daejeon 305–350, Republic of Korea*
[2]*Radio Technology Research Department, Electronics and Telecommunications Research Institute, 218 Gajeongno, Yuseong-gu, Daejeon 305-700, Republic of Korea*
✉ *E-mail: syeom@etri.re.kr*

Abstract: An orthogonally polarised stacked square microstrip patch array antenna structure with high-isolation performance is proposed for single channel full duplex wireless communications. A double symmetric microstrip array structure is collaborated with a special self-interference cancelling network called differential feeding network (DFN) in order to achieve high-isolation performance. The proposed 2 × 2 and 4 × 4 symmetric array antenna structures with the DFNs were designed to operate at the idustrial, scientific and medical band of 2.34–2.54 GHz. By measurement, the average isolation performances of 53 and 60.7 dB were obtained in 200 MHz frequency band by the 2 × 2 and 4 × 4 array antennas, respectively. The measured average gains of the 2 × 2 and 4 × 4 array antennas were found to be 14.4 and 19.4 dBi, respectively.

1 Introduction

A single channel full duplex (SCFD) wireless system effectively utilises both time and frequency resources as compared with time-division duplexing and frequency-division duplexing systems by simultaneously transmitting and receiving radio signals on the same frequency channel. However, the SCFD wireless has not been in widespread use because of a debilitating effect of self-interference which is presence of high-power leaked signals at the receiver from its own transmitter causing serious problems in the sensitive Rx-channel such as device saturation and failure to retrieve the received signals of interest [1]. In general, the self-interference should be suppressed to a system noise floor to obtain full benefit out from the SCFD transmission.

The self-interference can be suppressed at three different stages in a wireless system, and the techniques are known as antenna cancellation, radio-frequency/analogue cancellation and digital base-band cancellation. Among all three techniques, an effective antenna cancellation is the most essential prerequisite because an analogue cancellation alone cannot provide enough cancellation to prevent saturation of active components such as low noise amplifier and analog-to-digital converter prior to a digital base-band cancellation. Antenna separation is one of the antenna cancellation techniques, and it requires several antennas and thus more space [1, 2]. More advanced cancellation techniques include orthogonally polarised single antennas with improved feeding methods [3, 4], co-located antennas with a beam-forming feed network [5, 6] and orthogonally polarised microstrip array antennas with sequentially rotated array elements [7, 8]. A key technique employed in [1–8] to improve the self-interference cancellation (SIC) performance is adopting a self-induced destructive interference method. Array and co-located antenna structures such as in [5–8] have advantages to offer enough room to implement a SIC network, and perform the cancellation recursively as array size increases.

In this paper, we propose a unique high-isolation antenna structure where a double symmetric microstrip array is collaborated with a special feeding network called differential feeding network (DFN). The introduced transmit and receive (TRx) DFNs offer two times SICs in addition to the inherent isolation performance of the array elements.

2 Self-interference analysis in 2 × 2 dual-fed microstrip arrays

Self-interference in a TRx array antenna occurs because of the insufficient TRx isolation characteristic of an array element and the mutual couplings between the array elements. Spacing between the array elements and array geometric configuration determines the strength of spatial couplings in the array, whereas the TRx isolation of the array element determines the direct coupling. In Figs. 1*a* and *b*, asymmetric and symmetric configurations for a 2 × 2 array are depicted. As an array element, a dual feed stacked square microstrip patch antenna with orthogonal linear polarisations as shown in Fig. 1*c* was chosen. Both arrays were designed at the industrial, scientific and medical (ISM) band of 2.34–2.54 GHz and each array element was directly fed with a required current distribution (amplitude and phase) to form a high gain directional beam at the boresight. The simulated mutual coupling parameters (by computer simulation technology Microwave Studio™ 2010) at the R_1, Rx-port of the array element 1, are shown in Fig 2.

From the simulation results shown in Figs. 2 *a* and *b*, it is observed that the direct coupling $C_{R_1T_1}$ and the spatial coupling from the diagonal element $C_{R_1T_3}$ are stronger than the spatial couplings from the adjacent elements, $C_{R_1T_2}$ and $C_{R_1T_4}$ in both asymmetric and symmetric arrays. In general, all four coupling parameters in the asymmetric array are different from each other, whereas the coupling parameters $C_{R_1T_2}$ and $C_{R_1T_4}$ in the symmetric array are exactly same. Moreover, coupling parameters at the other Rx-ports R_2, R_3 and R_4 of the symmetric array will be as same as those at R_1 because of its double symmetric structure in both OX and OY planes. However, it is not true in the asymmetric array.

To achieve high-isolation between TRx-ports of an array, those unwanted coupled signals, especially the direct coupling signal, at each Rx-port of the array elements should be effectively suppressed. In that respect, the symmetric array is best to use because each coupled signal has its counterpart (a signal with same power and/or same phase) at other ports, and simply adding them destructively in an Rx combining network would result in higher isolation. Therefore a feeding network which not only feeds the array and combines the received signals, but also cancels out any coupled Tx-signals at the Rx-port is necessary to achieve high-isolation performance in array antennas.

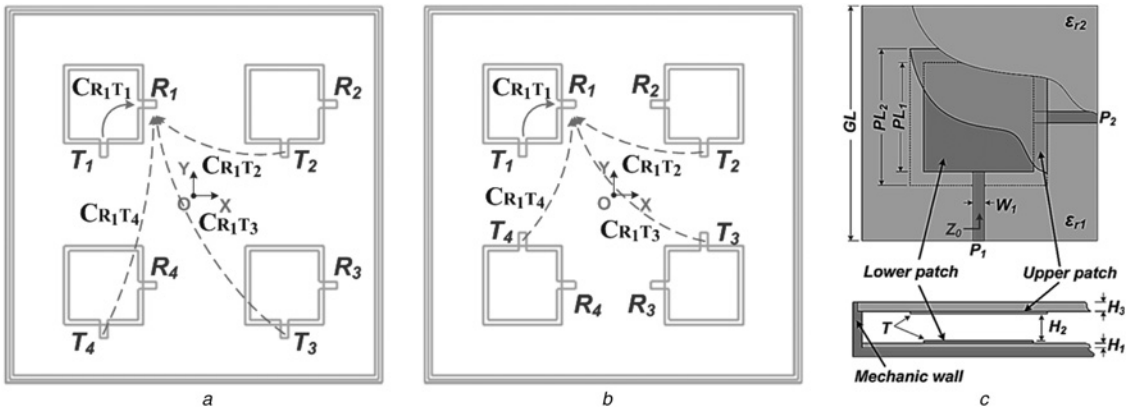

Fig. 1 *2 × 2 Array configurations*

a Conventional asymmetric array
b Mirrored symmetric array
c Single array element structure ($PL_1 = 38.3$ mm, $PL_2 = 43.5$ mm, $H_1 = 0.508$ mm, $H_2 = 6.5$ mm, $H_3 = 1.6$ mm, $W_1 = 4.2$ mm, $\varepsilon_{r1} = 2.6$(TLY7), $\varepsilon_{r2} = 4.4$(FR4), $GL = 100$ mm and $Z_0 = 20.5\ \Omega$)

3 Proposed 2 × 2 symmetric array antenna with DFNs

A special orientation of the array elements in the 2 × 2 symmetric array requires same amplitude, but 180° relative phase difference between the opposing Tx-ports to combine the radiated signals in free space and to form a high gain directional beam. Similarly, 180° relative phase difference between the opposing Rx-ports is required to combine the received signals in-phase. To meet the required 180° phase difference in both transmitting and receiving, a special feed network called DFN was proposed as a Tx- and Rx-feed network. Both TRx-DFNs use T-junctions with equal power split and simple 180° delay lines, thus narrowband operation is provided.

The proposed narrow band (NB)-DFNs integrated into the 2 × 2 symmetric array is depicted in Fig. 3*a*, whereas a block diagram of the overall structure for analysis is shown in Fig. 3*b*.

For the simplified isolation analysis between the TRx-ports of the proposed 2 × 2 array, we assume that the feeding network is lossless and no spatial couplings between the feeding network and the radiating elements.

If an incident signal $a_{\text{in},T_x} = A\cos(\omega t)$ is given at the Tx-input port ①, it is distributed by the Tx-DFN as shown in Fig. 3*b* and the delivered signal at each Tx-port ② of the array elements can be represented by the following (1)

$$a_{\text{in},T_i} = \alpha_{\text{in},T_i}\sqrt{1-|\Gamma_{\text{in}}|^2}\,a_{\text{in},T_x} \quad i = 1,\ 2,\ 3,\ 4 \tag{1}$$

where Γ_{in} is the reflection coefficient of Tx-DFN at the input port of the 2 × 2 array, whereas α_{in,T_i} is a transmission coefficient of the lossless Tx-DFN, defining the amplitude and phase distribution by the network for a T_i port of the array. Four transmission coefficients have following properties and relationship

$$\left|\alpha_{\text{in},T_i}\right|^2 = \frac{1}{4}, \quad i = 1,\ 2,\ 3,\ 4 \tag{2.1}$$

$$\begin{aligned}\Delta\theta &= \left|\text{ang}(\alpha_{\text{in},T_1}) - \text{ang}(\alpha_{\text{in},T_4})\right| \\ &= \left|\text{ang}(\alpha_{\text{in},T_2}) - \text{ang}(\alpha_{\text{in},T_3})\right| = \pi\frac{f}{f_c}\end{aligned} \tag{2.2}$$

$$\alpha_{\text{in},T_1} = \alpha_{\text{in},T_2},\ \alpha_{\text{in},T_3} = \alpha_{\text{in},T_4} \tag{2.3}$$

The Tx-DFN divides the input power equally between four array elements, but delays the signals to the array elements 3 and 4 by 180°(or π) respect to the signals to the elements 1 and 4 as seen from (2.1) and (2.2), respectively. From (2.2), 180° relative phase delay is exact only at f_c, and deviates as frequency changes.

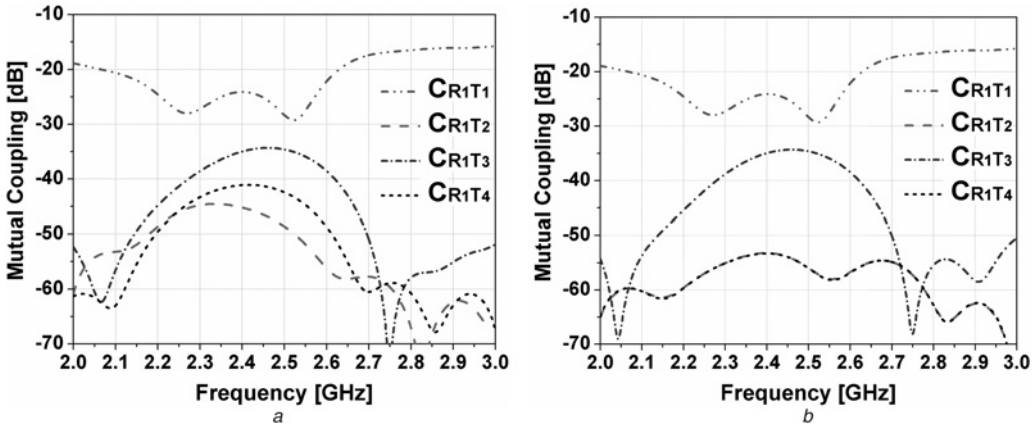

Fig. 2 *Simulation results of*

a 2 × 2 Asymmetric array
b 2 × 2 Symmetric array

IET Microw. Antennas Propag., 2015, Vol. 9, Iss. 11, pp. 1113–1119

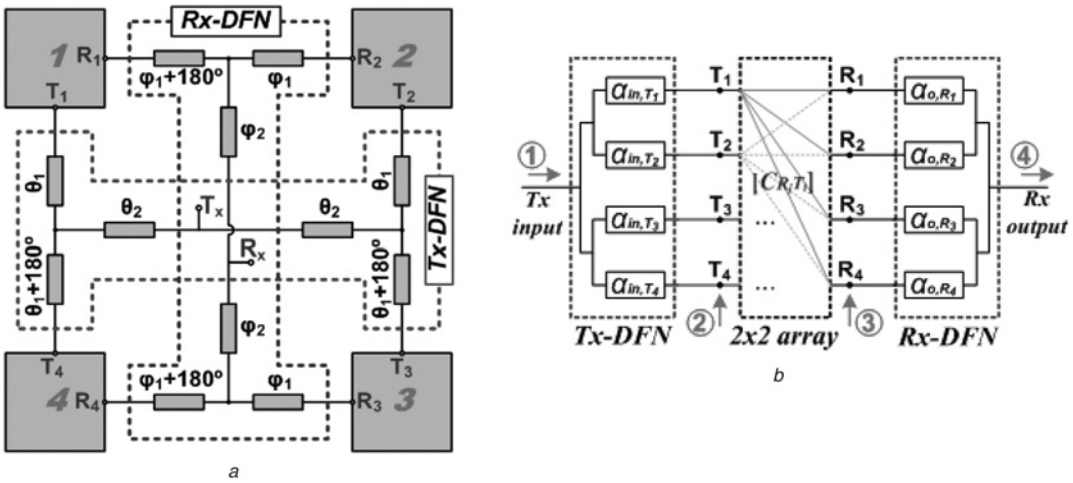

Fig. 3 *Proposed 2 × 2 symmetric array with NB-DFNs*

a Conceptual drawing
b Block diagram

Equation (2.3) shows relationships between the transmission coefficients.

The Tx-signals, a_{in,T_i}, are then radiated by the array elements, but still some small powers are coupled to Rx-ports ③ of the array and they are described by

$$b_{o,R_j} = \sum_{i=1}^{4} C_{R_jT_i} a_{\text{in},T_i} \qquad j = 1,\ 2,\ 3,\ 4 \tag{3}$$

where $C_{R_jT_i}$ represents mutual coupling fields within the 2 × 2 symmetric array and comprised into the coupling matrix as below

$$C_{R_jT_i} = \begin{bmatrix} C_{R_1T_1} & C_{R_1T_2} & C_{R_1T_3} & C_{R_1T_4} \\ C_{R_2T_1} & C_{R_2T_2} & C_{R_2T_3} & C_{R_2T_4} \\ C_{R_3T_1} & C_{R_3T_2} & C_{R_3T_3} & C_{R_3T_4} \\ C_{R_4T_1} & C_{R_4T_4} & C_{R_4T_3} & C_{R_4T_4} \end{bmatrix} \tag{4}$$

The coupling parameters in diagonal, highlighted in yellow, are direct coupling parameters and all have the same power as $C_{R_1T_1} \geq 24.1$ dB as read from Fig. 2*b*. The parameters highlighted in blue colour are spatial couplings between the adjacent elements and all have same power as $C_{R_1T_2} = C_{R_1T_4} \geq 53.25$ dB. The spatial coupling between the diagonal elements are highlighted in red colour and all have same power as $C_{R_1T_3} \geq 34.3$ dB.

And finally, the coupled Tx-signals along with the received Rx-signals are combined by the Rx-DFN. Although Rx-signals are combined in-phase, coupled Tx-signals will be cancelled out. The total Tx-signal at the output Rx-port ④ of the array can be represented by

$$b_{o,R_x} = \sum_{j=1}^{4} \alpha_{o,R_j} b_{o,R_j} \tag{5}$$

where α_{o,R_j} is the transmission coefficient of the lossless Rx-DFN and the relationships between the coefficients are

$$\left|\alpha_{o,R_j}\right|^2 = \frac{1}{4} \qquad j = 1,\ 2,\ 3,\ 4 \tag{6.1}$$

$$\begin{aligned} \Delta\varphi &= \left|\text{ang}(\alpha_{o,R_1}) - \text{ang}(\alpha_{o,R_2})\right| \\ &= \left|\text{ang}(\alpha_{o,R_3}) - \text{ang}(\alpha_{o,R_4})\right| = \pi \cdot \frac{f}{f_c} \end{aligned} \tag{6.2}$$

$$\alpha_{o,R_1} = \alpha_{o,R_4} \quad \alpha_{o,R_2} = \alpha_{o,R_3} \tag{6.3}$$

As referring to Fig. 3 and (2.2) and (6.2), it is evident that cancellations for the coupled Tx-signals with same amplitude will occur at the first combining points of the Rx-DFN because of $\Delta\varphi$, and again at the second (the final) combining point of the Rx-DFN because of $\Delta\theta$. The TRx-DFNs therefore provide two times SICs to the 2 × 2 array.

The operational bandwidth of the proposed high-isolation 2 × 2 array is determined by the impedance bandwidth of the array elements, a phase error in the TRx-DFNs and the input/output matching of the array. The phase error (amount of phase deviation from 180°) in the TRx-DFNs is caused by phase dispersion over frequency because of the simple delay lines. From (2.2) and (6.2), the maximum phase error of the TRx-DFNs within the operating band of 2.34–2.54 GHz is ±7.4°.If we assume no error in amplitude and maximally ±7.4° error in phase, at least 23 dB cancellation can be obtained at each time of combining in the Rx-DFN in addition to inherent isolation between the TRx-ports of the array element. Therefore we expect to achieve as high as 70 dB isolation performance in the proposed 2 × 2 array antenna, that is, 24 dB from the inherent isolation of the stacked microstrip element plus 46 dB from the two times cancellation in the TRx-DFN. Moreover, if we extend the array into 4 × 4 and employ another TRx-DFNs, theoretically it is possible to achieve ultra-high isolation over 110 dB. In practice however, it is impossible to achieve such ultra-high-isolation because of unpredictable conditions such as mutual couplings by leakage or surface current between the TRx-feed networks, and other asymmetrical scatterings or reflections from the mechanic or the radome.

For broadband (BB) applications, we also propose a BB-DFN using a BB phase shifter with 45° open/short-stubs. The BB phase shifter with 45° open/short-stubs proposed in [9] can provide 180° relative phase shift over 50% fractional bandwidth with ±2° phase deviation for voltage standing wave ratio = 1.15:1.The conceptual drawing of the BB-DFNs integrated into the 2 × 2 symmetric array is shown in Fig. 4.

The power delivered at the J_1 T-junction is equally divided between the path 1 and path 2. The path 1 is a simple microstrip transmission line with a characteristic impedance of Z_1 and an electrical length which is relatively 180° longer than the path 2, that is, $\varphi_m + 180°$. The path 1 has a normal phase dispersion property over frequency. On the other hand, the path 2 consists of a fixed main line with a length of $\varphi_m = 180°$ and two double open/short-stubs with an electrical length of $\varphi_s = 45°$. The phase slope of the path 2 is controlled by the specific values of Z_m and Z_s in

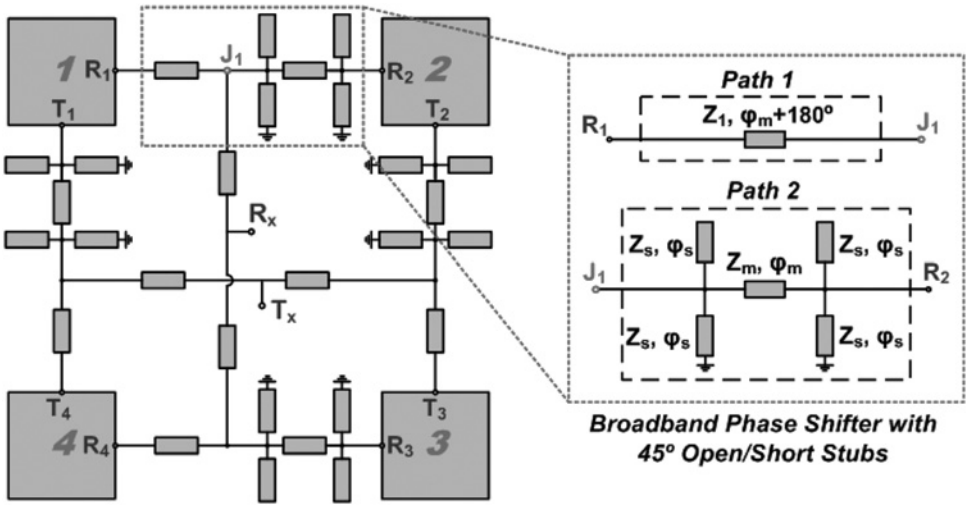

Fig. 4 *Drawing of 2 × 2 symmetric array with BB-DFNs*

order to align with the phase slope of the path 1 for keeping the desired 180° relative phase difference over wide-frequency band with a minimum phase error. The designing procedure of the BB phase shifter can be found in [9]. For the operating band of 2.34–2.54 GHz and the port impedance of 50 Ω, the BB phase shifter with the optimised parameters of $Z_1 = 50\,\Omega$, $Z_m = 80.8\,\Omega$, $\varphi_m = 180°$, $Z_s = 62.78\,\Omega$, $\varphi_s = 45°$ gives 180° relative phase difference with ±1° phase error between the path 1 and path 2. As compared with the NB-DFNs shown in Fig. 3, the BB-DFN shown in Fig. 4 ensures very small phase error of ±1° over the operating band, but requires more room to be implemented. A high-impedance design or multilayer design could be a solution to employ the BB-DFNs into the 2 × 2 array structure.

4 Antenna fabrication and measurement

To check the feasibility of the proposed structures for high-isolation performance, we fabricated the 2 × 2 symmetric array with the NB-DFNs. The 2 × 2 array antenna was realised on TLY-7 substrate ($\varepsilon_r = 2.6$, $H_{TLY} = 0.508$ mm, $T = 0.018$ mm, $\tan\delta = 0.002$ at 2 GHz) and shown in Fig. 5*a*. The parasitic patches were realised on a flame retardant 4 (FR4) substrate ($\varepsilon_r = 4.4$, $H_{FR} = 1.6$, $T = 0.018$ mm, $\tan\delta = 0.025$ at 2 GHz) as shown in Fig. 5*b* and were placed at the height of 6.5 mm over the active patches by the support of the mechanic wall-edge. The 2 × 2 array is matched at both the TRx-ports with 50 Ω.

Furthermore, a 4 × 4 array was assembled by using the 2 × 2 array as a sub-array to examine if additional BB TRx-DFNs could further improve the isolation performance as we expected. The front-view of the 4 × 4 array antenna with the stacked patches removed is shown in Fig. 6 *a*, whereas the back-view of the array, where TRx-ports of the sub-arrays are connected to the BB-DFNs by50 Ω flexible coaxial cables with a length of 20 cm (RG141) and subminiature version A connectors, is shown in Fig. 6*b*. For symmetry, the sub-arrays in the 4 × 4 array antenna are placed in mirror to each other as the orientation of the single elements in the 2 × 2 array. The BB-DFNs of the 4 × 4 array were fabricated on the same TLY-7 substrate and placed in a separate mechanic box as shown in Fig. 6*b*. All ports of the BB-DFN are matched with 50 Ω. The electrical design parameters given in Section 3 were used.

The simulated return loss (RL) and isolation (Iso) performances of the proposed 2 × 2 array antenna are given in Fig. 7*a*, whereas the measured performances of the 2 × 2 and 4 × 4 array antennas are compared in Fig. 7*b*. By simulation, the proposed 2 × 2 array antenna structure achieved the isolation performance of 57.2 dB at minimum and 60.4 dB in average within the operating band, whereas the expected isolation performance was 70 dB. The simulated isolation performance below the expected value reveals that unpredicted mutual couplings do exist between the TRx-DFNs because of the same layer and unshielded feeding network structure. In other words, the Tx-DFN is on the same layer as Rx-DFN, and thus Tx-signals can be coupled to the Rx-DFN through the surface current and/or spurious radiations yielded by

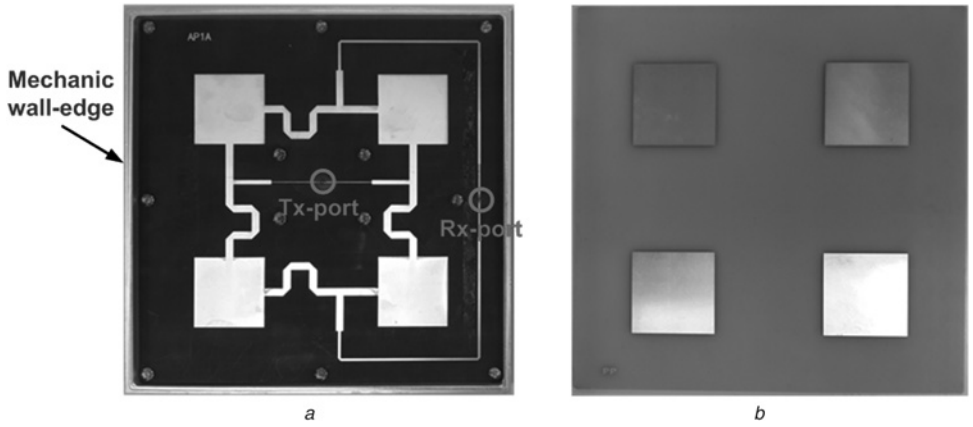

Fig. 5 *Fabricated 2 × 2 array*

a Front-view
b Parasitic patches realised on FR4 substrate

IET Microw. Antennas Propag., 2015, Vol. 9, Iss. 11, pp. 1113–1119

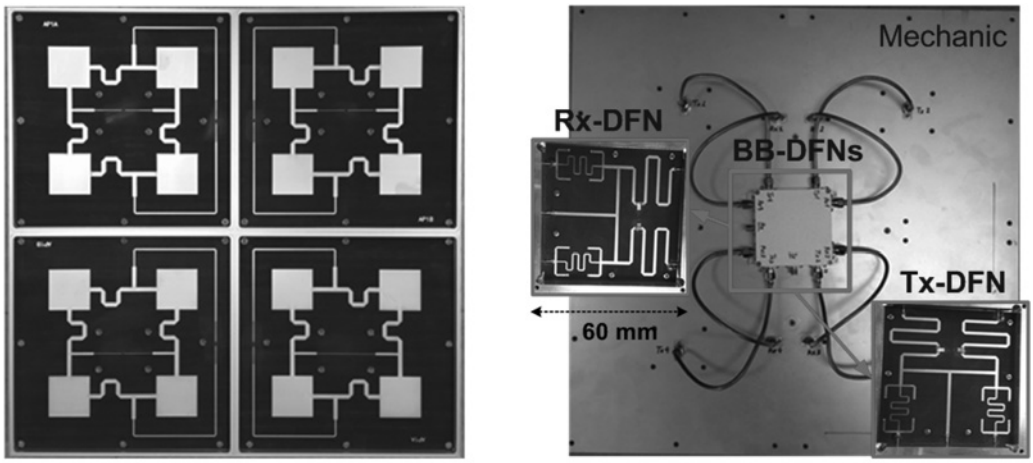

Fig. 6 *Fabricated 4 × 4 array*

a Front-view (parasitic patches are not shown)
b Back-view (BB-DFNs are connected to the 4 × 4 array)

the bending elements and discontinuities in the Tx-DFN. Mutual couplings between the array elements and the feed networks may also contribute to the performance degradation.

From the measurement results given in Fig. 7*b*, the isolation performance of the 2 × 2 array was obtained as 51 dB at minimum and 53 dB in average within the operating band. On the other hand, the isolation performance of the 4 × 4 array was 56.7 dB at minimum and 60.7 dB in average. As compared with the isolation performance of the 2 × 2 array, the isolation improvement of only 7.7 dB in average and maximally 12.4 dB was achieved by the 4 × 4 array antenna despite the employment of additional BB TRx-DFNs. Potential fabrication errors and assembling errors do adversely affect the balanced current distribution over array elements and consequently degrading the interference cancellation performance of the DFNs, especially in the 4 × 4 array because of the use of additional coaxial cables and SMA connectors. Moreover, mutual couplings between the 2 × 2 sub-arrays do also exist in the 4 × 4 array structure and restrict the isolation performance to a certain fixed value. Both fabricated 2 × 2 and 4 × 4 array antennas were well matched within the operating band with more than 10 dB RL.

In general, we conclude that the simple, single layer, co-planar structure of the proposed array antennas caused unpredicted, non-symmetrical mutual couplings between the Tx and Rx feeding networks as well as between the feeding networks and the array elements which consequently degraded the interference cancellation performance of the DFNs and resulted in lower isolation performance than the expected. Therefore in order to achieve high-isolation performance by the proposed structures, we should perfectly isolate TRx-DFNs from each other as well as from the radiating elements by using a multilayer structure and/or shielding the feed networks with metallic walls.

The radiation pattern performances of the fabricated 2 × 2 and 4 × 4 arrays were measured in an anechoic chamber. The measured *E*- and *H*-plane radiation patterns at the centre frequency are shown in Fig. 8, whereas the detailed radiation parameters at three frequencies, that is, 2.34, 2.44 and 2.54 GHz, are summarised in Table 1. As shown in Fig. 8, both array antennas have directional beams at the boresight. However, maximally ±2° beam offset was found in the radiation patterns of the 2 × 2 array antenna because of the phase dispersion in the NB-DFNs. In other words, the simple 180° phase delay lines employed in the NB-DFNs gave ±7.4° phase error within the operating band as mentioned in Section 3, and that phase error was subsequently resulted in ±2° beam offset. If the BB-DFNs were employed in the 2 × 2 symmetric array as shown in Fig. 4, the phase error would be bounded within ±1° over the operating band, and thus the beam offset problem could be eliminated. On the other hand, beam offset in the 2 × 2 array is naturally compensated by the mirror arrangement of 2 × 2 sub-arrays in the 4 × 4 array. Moreover, the

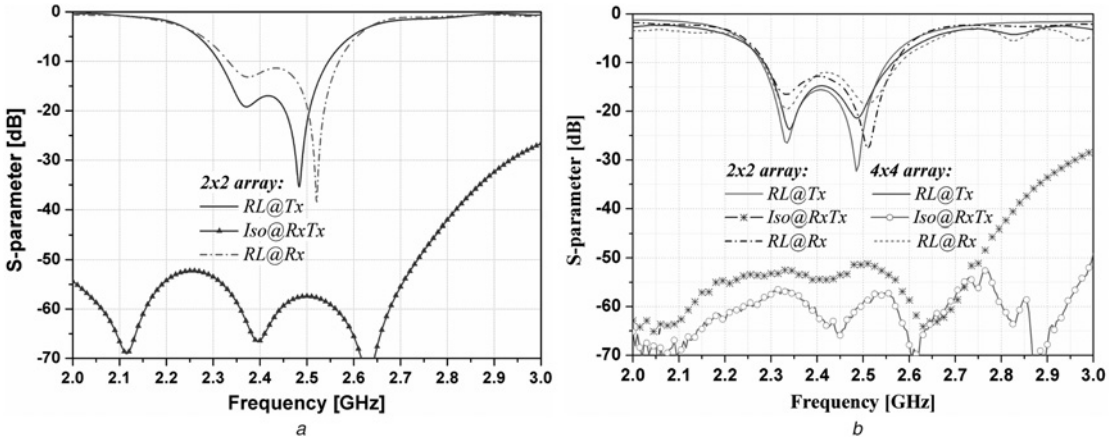

Fig. 7 *Result comparisons*

a Simulation results of the 2 × 2 array
b Measurement results of the 2 × 2 and 4 × 4 arrays

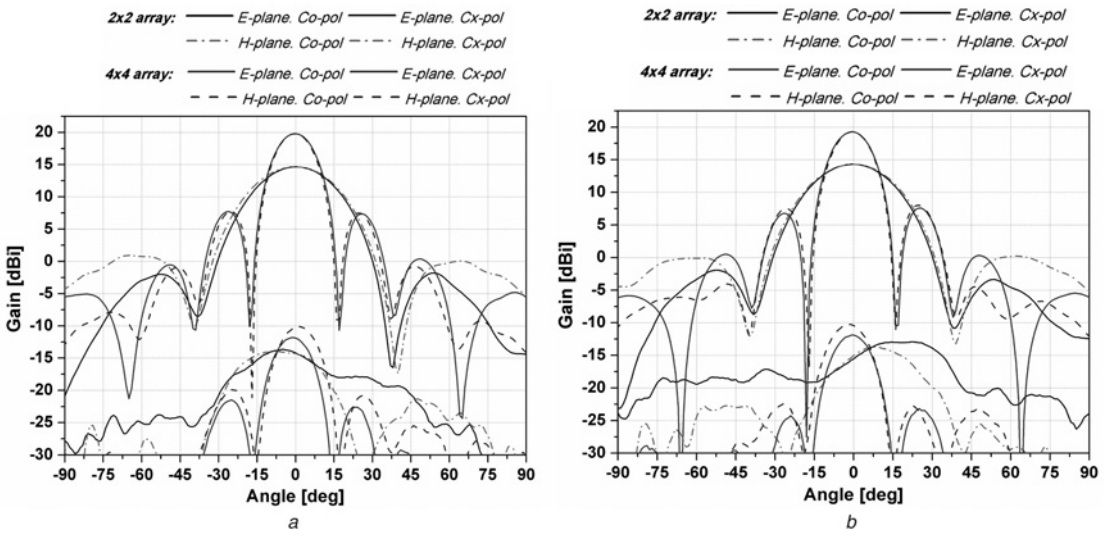

Fig. 8 *Compared radiation patterns of 2 × 2 and 4 × 4 arrays (at f = 2.44 GHz) measured at*

a Tx-port
b Rx-port

Table 1 Summarised radiation parameters

Frequency, GHz	Port	Gain, dBi		Cross-polarisation level, dBc				Sidelobe level, dBc			
		2 × 2 array	4 × 4 array	2 × 2 array		4 × 4 array		2 × 2 array		4 × 4 array	
				E-plane	*H*-plane	*E*-plane	*H*-plane	*E*-plane	*H*-plane	*E*-plane	*H*-plane
2.34	Tx	14.43	19.49	30.18	28.93	31.08	34.39	15.85	14.39	11.90	12.58
	Rx	14.10	19.25	31.28	28.41	31.93	35.32	14.81	14.10	12.61	13.03
2.44	Tx	14.66	19.80	26.77	26.25	31.21	28.82	16.45	13.72	12.09	12.03
	Rx	14.30	19.26	24.25	25.77	31.16	28.32	16.23	14.08	11.65	11.24
2.54	Tx	14.60	19.60	27.32	26.03	30.19	32.32	17.57	12.58	12.22	12.31
	Rx	14.22	19.16	27.24	29.33	29.58	33.35	15.03	12.15	12.02	12.26

Note: the measured gains are the beam peak values.

use of BB-DFNs as a combining network for the sub-arrays minimises the potential beam offset in the 4 × 4 array.

The measured gains of the 2 × 2 array antenna at the centre frequency are 14.66 dBi at the Tx-port and 14.3 dBi at the Rx-port. For the 4 × 4 array antenna, the measured gains are 19.8 dBi at the Tx-port and 19.26 dBi at the Rx-port. As observed from the gain information given in Table 1, the measured gain of the 2 × 2 array at the Rx-port is about 0.35 dB lower than that at the Tx-port because of the longer transmission lines employed in the Rx-DFN in order to avoid direct crossing with the transmission lines in the Tx-DFN. For the same reason, about 0.4 dB gain difference was found between the radiation patterns measured at the Tx- and Rx-ports of the 4 × 4 array antenna. When compared the gain performances of the 2 × 2 and 4 × 4 array antennas, the average gain increment obtained by the 4 × 4 array is calculated as 5.1 dB and which is found to be acceptable when a feeder loss from the BB-DFNs including the 20 cm long coaxial cables and SMA connectors used in the 4 × 4 array is taken into account. By a separate measurement of the BB-DFNs and the 20 cm long coaxial cables, the feeder loss in the 4 × 4 array was found to be 0.7–1 dB over the operating band of 2.34–2.54 GHz.

The cross-polarisation level performances of both the array antennas were found to be acceptable. The average cross-polarisation levels for the 2 × 2 and 4 × 4 array antennas are 27.65 and 31.47 dBc, respectively.

The average sidelobe levels of the 2 × 2 array antenna are 15.9 dB cat *E*-plane and 13.5 dBc at *H*-plane. For the 4 × 4 array antenna, the average sidelobe levels are 12.1 dBc at *E*-plane and 12.2 dBc at *H*-plane. A little discrepancy found between the *E*- and *H*-plane sidelobe level measurements of the 2 × 2 array is because of the asymmetric spurious radiations from the feeding network, that is, the bended 180° delay lines. In contrast, similar sidelobe level characteristics were found at *E*- and *H*-plane measurements of the 4 × 4 array because of the complementary spurious radiations from the symmetric feeding networks.

5 Conclusion

Double symmetric microstrip 2 × 2 and 4 × 4 array antennas with high-isolation performance were proposed in this paper. Narrowband and BB-DFNs were employed for the additional SIC function. The fabricated 2 × 2 and 4 × 4 array antennas achieved the average isolation performances of 53 and 60.7 dB in 200 MHz frequency band, respectively. The employment of the BB-DFN in the 4 × 4 array minimises the beam peak offset in addition to BB impedance matching and maximum SIC performance. The necessity of the BB-DFN will be more evident in case of BB design. As future work, we will improve the proposed structure by making necessary modifications that we found through this study, for example, isolate the TRx feeding networks from each other as well as from the radiating elements by employing a multilayer and shielded transmission line structures. Moreover, we will design the BB-DFN in small form in order to employ it in a 2 × 2 array where design space is limited using an embedded module such as

IET Microw. Antennas Propag., 2015, Vol. 9, Iss. 11, pp. 1113–1119

low temperature co-fired ceramic chip or a substrate with a high dielectric constant value.

References

1 Choi, J.I., Jain, M., Srinivasan, K., *et al.*: 'Achieving single channel, full duplex wireless communication'. Mobicom'10, IL, USA, September 2010, pp. 1–12
2 Wegener, A.T., Chappell, W.J.: 'Simultaneous transmit and receive with a small planar array'. 2012 IEEE MTT-S Int. Microwave Symp. Digest (MTT), June 2012, pp. 1–3
3 Xie, J.J., Yin, Y.Z., Wang, J.H., Liu, X.L.: 'Wideband dual-polarized electromagnetic fed patch antenna with high isolation and low cross-polarization', *Electron. Lett.*, 2013, **49**, (3), pp. 171–173
4 Luo, K., Ding, W., Hu, Y., Cao, W.: 'Design of dual-feed dual-polarized microstrip antenna with high isolation and low cross polarization', *Prog. Electromagn. Res. Lett.*, 2013, **36**, pp. 31–40
5 Moulder, W.F., Perry, B.T., Herd, J.S.: 'Wideband antenna array for simultaneous transmit and receive (STAR) applications'. APS/URSI 2014, TN, USA, July 2014, pp. 243–244
6 Fenn, A.J., Hurst, P.T., Herd, J.S., *et al.*: 'Simultaneous transmit and receive antenna system'. US Patent 2013/0106667 A1, May 2013
7 Jang, H.S., Lim, W.G., Son, W.I., *et al.*: 'Microstrip patch array antenna with high isolation characteristic', *Microw. Opt. Technol. Lett.*, 2012, **54**, (4), pp. 973–976
8 Hall, P.S.: 'Dual circularly polarized sequentially rotated microstrip array with high isolation', *Microw. Opt. Technol. Lett.*, 1992, **5**, (5), pp. 236–239
9 Eom, S.Y., Park, H.K.: 'New switched-network phase shifter with broadband characteristics', *Microw. Opt. Technol. Lett.*, 2003, **38**, (4), pp. 255–257